THE INVESTIGATION OF FATIGUE LIFE IN A 6061-T6 ALUMINUM BICYCLE FRAME

by

RAYMOND C. IZOR

Submitted in Partial Fulfillment
of the Requirements for the
Degree of Bachelor of Science
in Mechanical Engineering
at the
MASSACHUSETTS INSTITUTE OF TECHNOLOGY
May, 1975

Signature of Author. Signature redacted

Certified by. Signature redacted
Thesis Supervisor

Accepted by . Signature redacted
Chairman, Departmental Committee on Theses

ARCHIVES
MASS. INST. TECH
MAR 15 1976
LIBRARIES

THE INVESTIGATION OF FATIGUE LIFE

IN A 6061-T6 ALUMINUM BICYCLE FRAME

by

RAYMOND C. IZOR

Theses
TM
1975
I29

Submitted in Partial Fulfillment

of the Requirements for the

Degree of Bachelor of Science

in Mechanical Engineering

at the

MASSACHUSETTS INSTITUTE OF TECHNOLOGY

May, 1975

Signature of Author. . . . . .

Certified by. . . . . Thesis Supervisor

Accepted by . . . . . Chairman, Departmental Committee on Theses

ARCHIVES
MAR 15 1976
LIBRARIES

ACKNOWLEDGEMENTS

The subject of this thesis, namely the investigation of failure by fatigue of a 6061-T6 aluminum bicycle frame, was originally proposed by Professor Shawn Buckley.

I also take this opportunity to express my appreciation for financial support from the Richard C. McCurdy Fund for Undergraduate Research.

Table of Contents

Acknowledgements. 1

Abstract. 3

Table 1, Marketed Frames Comparison 17

List of Figures 4

Introduction

Bicycles 5

Fatigue. 6

Apparatus and Procedure

Pointer System 10

Loading Mechanism. 12

Results and Reccomendations 15

Appendix 1, Nomenclature. 35

Appendix 2, Maximum Tube Deflection Analysis

a) Seat Tube 36

b) Down Tube 36

Appendix 3, Power Requirement Analysis. 38

Bibliography. 39

ABSTRACT

One of the several new types of bicycle frames recently marketed is one produced by the Klein Company. It is made of 6061-T6 aluminum. This frame optimized the tradeoff between weight and rigidity. The area of uncertainty remained in its abilily to resist fatigue. The main objective of this thesis was to obtain some information on the frame's expected life by designing a system to simulate the rider and using it to test the frame. A device was developed which measured the deflection of the main tubes of the frame. The cyclic loading machine was then constructed to fatigue test the bicycle frame. The final result was the survival of the frame without crack initiation after 100,000 cycles of simulated pedaling.

LIST of FIGURES

Figure 1, Frame Nomenclature. 18

Figure 2, S-N Diagram for 6061-T6 Aluminum. 19

Figure 3, Goodman Diagram 19

Figure 4, Pointer System - Overall View 20

Figure 5, 6, 7, Pointer System - Detailed Views . 21 - 23

Figure 8, Pointer System - Exploded View. 24

Figure 9, Loading of Bottom Bracket

a) Rider Effected. 25

b) Machine Effected. 25

Figure 10, Simulating Mechanism - Overall View. 26

Figure 11, Handlebar Simulation 27

Figure 12, Spring Loading; Lever Arm Attachment. . . .28

Figure 13, Spring Loading 29

Figure 14, Spring Loading - Exploded View 30

Figure 15, Eccentric and Connecting Rod 31

Figure 16, Connecting Rod - Part One - Line Drawing . .32

Figure 17, Connecting Rod - Part Two - Line Drawing . .32

Figure 18, Eccentric - Line Drawing 33

Figure 19, Lever Arm Assembly - Exploded View 34

INTRODUCTION

Bicycles

With the recent escalation of interest in all modes of bicycling as a sport came a rejuvenation in the bicycle-making industry. Each component made headway in the development of better materials as well as mechanisms. This development was extended into the bicycle frame itself (see figure 1); new frames were made out of materials other than the traditional steel.

In optimizing the performance of a bicycle frame there are three constraining criteria: strength, rigidity, and weight. Unfortunately they are conflicting antagonists. The steel frame had been the ultimate product of the industry until recently. It represented the survival of the fittest, an evolutionary trial and error development of bicycles throughout their history. Recently however new possibilities came into the realm of feasible materials: plastic, titanium, aluminum, carbon fiber, and magnesium. Each material has its own problems, and some of these problems are common to more than one material. These problems are especially significant to either track or cross-country racing frames. The steel frame is too heavy, although the stiffest. The aluminum frame, by changing parameters, improves on the weight-stiffness tradeoff but is susceptible to fatigue. This problem is

remedied by heat treatment. Titanium frames are light and slightly less rigid, however they are acceptable. They are also difficult to join together which makes them relatively expensive. Plastic is the lightest but is too flexible. Magnesium is too brittle, capable of shattering on impact. Carbon fiber frames have a problem similar to the magnesium frame although research in the area may have overcome the obstacle since carbon fiber frames are now on the market. A comparison of the marketable frames is given in Table 1.

Klein Company, producers of a welded aluminum frame, have optimized the weight - rigidity tradeoff while keeping strength in the limelight of concern. The purpose of this thesis is to make a careful examination of one aspect of its strength, the mode of failure by fatigue.

Fatigue

Fatigue fracture resulting from cyclic deformation through a few cycles of large plastic strain is familiar to most people. This is called low cycle fatigue. The fact that failure can occur from many cycles at a small stress was not discovered until recently, when such demands were made of metal machinery. This type of fatigue can occur at stress levels much lower than the yield stress. This phenomenon is appropriately called high cycle fatigue.

The exact mechanism of fatigue failure is not completely known to date. However, some of the basic phenomena are known. First a crack must be formed where no crack originally existed, then it must grow in size to be sufficiently large to cause the part to fail. These are respectively called crack initiation and crack propagation.

Much of the mechanics of crack initiation is still in the dark, however this understanding has improved with the development of the concepts of the mechanisms of plastic deformation which followed the introduction of the dislocation theory. Recent advances in experimental techniques (such as electron microscopy) have contributed to the understanding as well.

In high cycle fatigue the stress amplitude is well below that of the yield stress, thus the strain is "purely elastic". In the light of high cycle fatigue this is an oversimplification introduced by the concept of yield stress. No material is perfectly elastic. The true situation is one in which there is a minute amount of plastic strain at even very low stresses. This is referred to as microstrain. Microstrain occurs inhomogeneously and it is believed that this eventually leads to crack initiation.

Once the crack has been initiated it propagates due to continuance of cyclic loading; the presence of the crack dominates the stress and strain behavior in the vicinity of the crack. Each cycle causes plastic deformation

at the tip of the crack, allowing the crack to propagate in a stepwise fashion. Since the extent of plastic deformation is a function of the stress amplitude it is not surprising that the number of cycles to failure is also a function of stress amplitude. This can be realized with the aid of the S-N diagram for 6061-T6 aluminum shown in figure 2. The S-N diagram is a graph on which alternating stress amplitude (σ_a) is plotted as a function of the number of cycles to failure. The S-N diagram shows that there is a stress below which fatigue is known not to occur. This stress is known as the fatigue limit. If the stress amplitude is below this value fatigue fracture will not occur.

For fatigue with positive mean stress one would employ the use of the Goodman diagram (figure 3). This diagram represents the theory that the life of the material is spent partly on cyclic loading, partly on mean loading. The Goodman diagram has been proven experimentally to increasingly underestimate the fatigue life with increasing mean stress. Thus it gives conservative estimates. The reason that the Goodman diagram is not used for negative mean stress is because a compressive mean stress either retards or has no effect on crack propagation. Therefore any influence which negative mean stress may exert is one of extending fatigue life rather than shortening it.

It is expected that a bicycle frame would fatigue fail at the bottom bracket weld. The reason for this is because crack initiation and propagation is accentuated by stress concentrations. Stress concentrations are caused by welding when the molten material cools at varying rates (dependent on distance from the quenching medium - usually air). The stress concentrations are relieved significantly by heat treatment, however they are not completely relieved. The welds remain the locations of greatest stress concentration. The bottom bracket is where the loading is applied, it also has several heavy welds. This makes it a prime target for fatigue failure.

APPARATUS and PROCEDURE

Pointer System

In order to insure that the cyclic loading device designed is accurately representative of the effect of a rider on the frame, a measuring system was needed to compare the two cases, real and simulated. It was decided that a device which allowed the bicycle to completely remain mobile was preferable to one which required the bicycle to remain motionless. Another requirement of the measuring system was that it be lightweight (so as not to significantly change the riding conditions). The suggested system was a set of three pointers to be mounted on the frame's three main tubes which support most of the load. The purpose of the pointers was to measure the tube deflections during pedaling in a manner similar to a torque wrench: the tube would deflect due to the bending and/or twisting moments exerted on it (induced by pedaling) while the pointer would remain essentially straight.

Thus the pointer system must a) be lightweight, b) be rigid in the direction of the tube deflection, c) have a spring loaded marker.

The final design and built system is shown mounted on the frame in figure 4 (overall view). Figures 5 - 7 give a detailed view of each pointer. Figure 8 is an

exploded view of one of the pointers which illustrates how they were constructed. The arm of the pointer is made of wood of rectangular cross-section which provides the necessary rigidity in the transverse direction. It is rigidly attached (glued and screwed) to a solid aluminum block. This block is attached (screwed) to two hose clamps; the clamps mount the system on a frame tube. The hose clamps are 1.5 inches apart, providing rigidity between the tube and the block while keeping the necessary sensitivity of deflection. On the opposite end of the pointer a pencil holder is mounted. Beneath this holder a small marking pad is clamped to the bicycle frame (see figure 7 for details). The springiness of the pointer in the direction perpendicular to that of the direction of tube deflection provides a "spring-loaded" pen which is adjustable.

In order to evaluate the pointer feasibility, an analysis of the maximum expected tube deflection was necessary. To achieve this result the seat and down tubes were each and individually modeled as cantilevers sustaining the entire load due to the expected bending moment. It was assumed that these two tubes would have a greater degree of deflection than the top tube since they are attached to the bottom bracket which induces the moment on the frame..

In the case of the seat tube the moment is a pure bending moment since the moment axis is a diameter of

the tube.

Since the beam's angular slope varies linearly with length, and deflection varies linearly with angular slope, it was possible to geometrically evaluate the deflection of one tube end relative to the other.

It was possible to analyze the down tube similarly. However this tube is under a combination of bending and twisting moments. The twisting moment (M_t) is equal to $M_o \cos 30^\circ$ (see figure 1); the bending moment (M_b) is equal to $M_o \sin 30^\circ$. The details of this analysis are given in appendices 1a, b. The results of this analysis are:

Maximum Deflection, Down Tube	2.4 in.
Maximum Deflection, Seat Tube	2.0 in.

Loading Mechanism

The simulation of the rider by a cyclic loading device must be relatively accurate. Before designing such a device consideration was made of the type of loading effected by a sprinter on his bike frame. There are only two locations of rider loading: the head tube and the bottom bracket (no force is applied at the seat since a racer is not normally on it - this is a luxury afforded only by tourists).

At the head tube one carries little body weight. The major effect is one of fixing the front of the frame with respect to the rider.

The loading of the bottom bracket is a slightly more complex case. It is assumed (reasonably so if one is experienced with bicycling) that the maximum force that a rider can exert on each pedal with his legs (in addition to his own body weight) is one half his body weight. It is also assumed these forces are applied at the center of the pedal. Thus the maximum loading condition which exists is shown in figure 9a. The loading condition that was proposed to apply to the frame during fatigue testing is shown in figure 9b. These two loading conditions give the same resultant force and moment on the bottom bracket.

The detailed design of this cyclic loading machine is illustrated with the aid of several figures. The bicycle frame is mounted horizontally, rather than vertically, on a machine bed. It was decided that the wheels would be left on rather than to attempt to simulate them with pivots at the front fork and rear dropout. The wheels rested against vertical supports which were bolted to the machine bed (see figure 10). The effect of the handlebars was simulated by bolting a one inch piece of steel pipe to the machine bed and clamping the fork stem to it (see figure 11). The simulation of the rider's weight was effected by looping steel cable around the bottom bracket axle and attaching one end of

a spring to it. The other end of the spring was hooked on an eyebolt which was drawn through a brace which, in-turn, was bolted to the machine bed. When the eyebolt was drawn, the spring was stretched, exerting a force on the axle. See figures 12 and 13 for details. Figure 14 gives an exploded view of the system.

Lastly and most importantly was the cyclic moment loading mechanism: A bicycle crank was bolted and clamped to one end of a lever arm 36 inches long. The opposite end of the lever arm was pinned to the inner race of a bearing mounted in a connecting rod. The two piece connecting rod length was variable due to the milled slots (see figure 15 for a photograph, figures 16 and 17 for line drawings). The other end of the connecting rod had its inner bearing race pinned to a motor driven eccentric. The eccentricity could be varied by moving the bearing's pivot point in the milled slot of the eccentric (see figure 15 for a photograph, figure 18 for a line drawing). See figure 19 for an exploded view of this mechanism.

An analysis of the power required to drive the cyclic moment mechanism was needed to determine the size (horsepower) motor needed to drive the system. Most of the power is required to accelerate the steel lever arm which is the only significant inertial mass. The results of the analysis gave a requirement of approximately one-tenth horsepower. The details of the analysis are given in appendix two.

RESULTS and RECOMMENDATIONS

The results of this thesis are twofold: First, the end product of the analysis and design of a rider simulating mechanism is illustrated in the accompanying figures. The simulation was one accurate enough to serve the ultimate purpose of the thesis. Second, the result of the test showed that the frame did not fail by fatigue after 100,000 cycles.

My recommendations are directed at achieving a more realistic loading and at determining the ultimate life of the frame. The simulation was accurate, but one alteration would significantly improve it. Mounting the lever arm perpendicular to the bottom bracket resulted in a shear force transmitted from the eccentric through the lever arm to the bottom bracket. This shear force is perpendicular to the plane of pedalling motion. Perhaps a slightly more realistic situation would be to mount the lever arm parallel to the pedal axis which would shift the direction of the shear force to the plane of the frame. Another modification I suggest in reference to the first recommendation relates to road conditions. Bicycles often cover rough road conditions (potholes, etc.) which could be simulated by having each wheel stop attached to a piston actuator which would have a displacement equal to average pothole depth. These

front and rear pistons could be triggered in sequence to simulate any speed desired.

To get a true estimate of the fatigue life of the frame I recommend utilization of the Goodman Criterion. The essence of this is written as

$$\frac{\sigma_a}{\sigma_{ao}} + \frac{\sigma_m}{\sigma_u} = 1$$

The major problem involved with this approach is the determination of the alternating and mean stresses in the frame. This requires an extensive stress analysis of the frame. If indeterminable, these stresses may be estimated with the use of strain gages mounted on the main tubes. From strain gage measurement the alternating and mean stresses can be determined. With this information the Goodman Criterion can be used. By running the fatigue test at a higher mean stress while keeping the alternating stress σ_a constant, σ_{ao} will increase, as a result the number of cycles to failure will be lowered enough to experimentally verify the fact that this point lies on the S-N curve for 6061-T6 aluminum.

Table 1

Actual Frame Weight and Stiffness[1]

Material	Manufacturer	Size: cm	Style	Weight: lb	Relative Stiffness
Steel	R. Schoeder*	55	Track	4.81	1.00
Titanium	Teledyne	58	Road	2.92	.76
Aluminum	Fabo-Alan	58	Road	3.31	.67
Aluminum	Klein	53	Track	3.31	2.14
Carbon Fiber	Mossberg**	--	Track	3.10	1.04

* This frame was used as a standard.

** From Mossberg data as presented in Bicycling using a similar stiffness test.

1. Buckley, Professor Shawn. Optimization of a Bicycle Frame

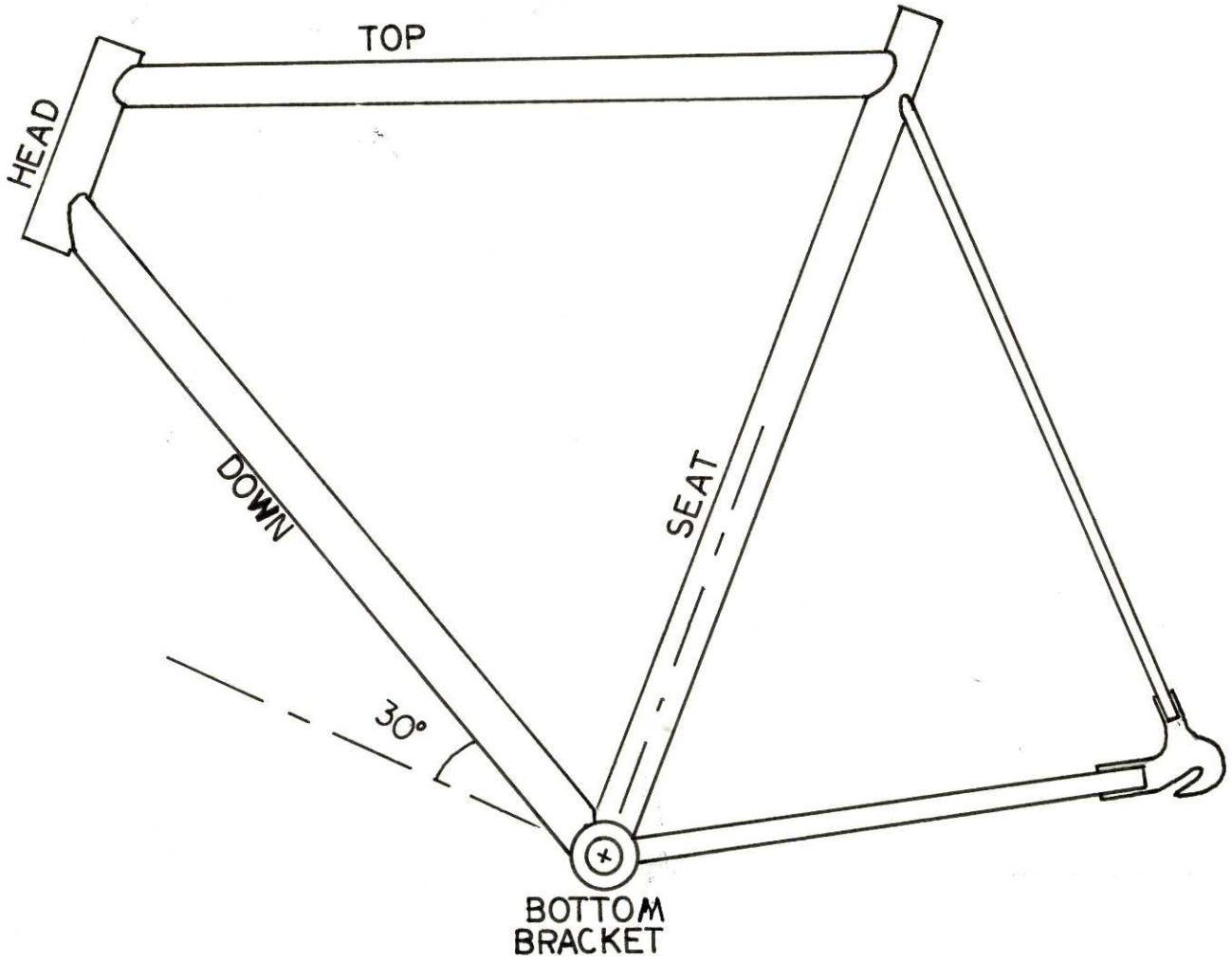

Frame Nomenclature

Figure 1

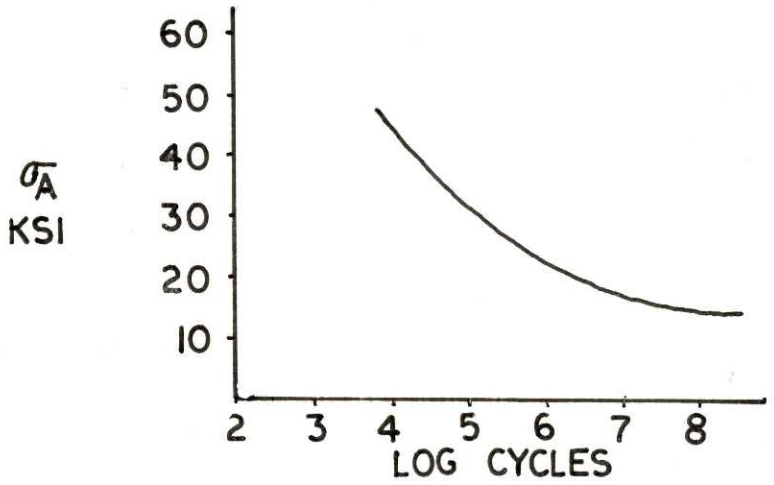

S-N Diagam for 6061-T6 Aluminum

Figure 2

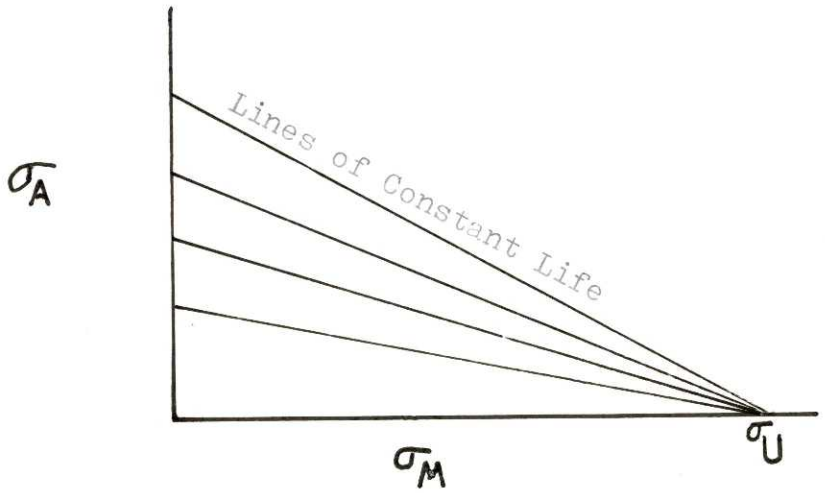

Goodman Diagram

Figure 3



Figure 4 Pointer System

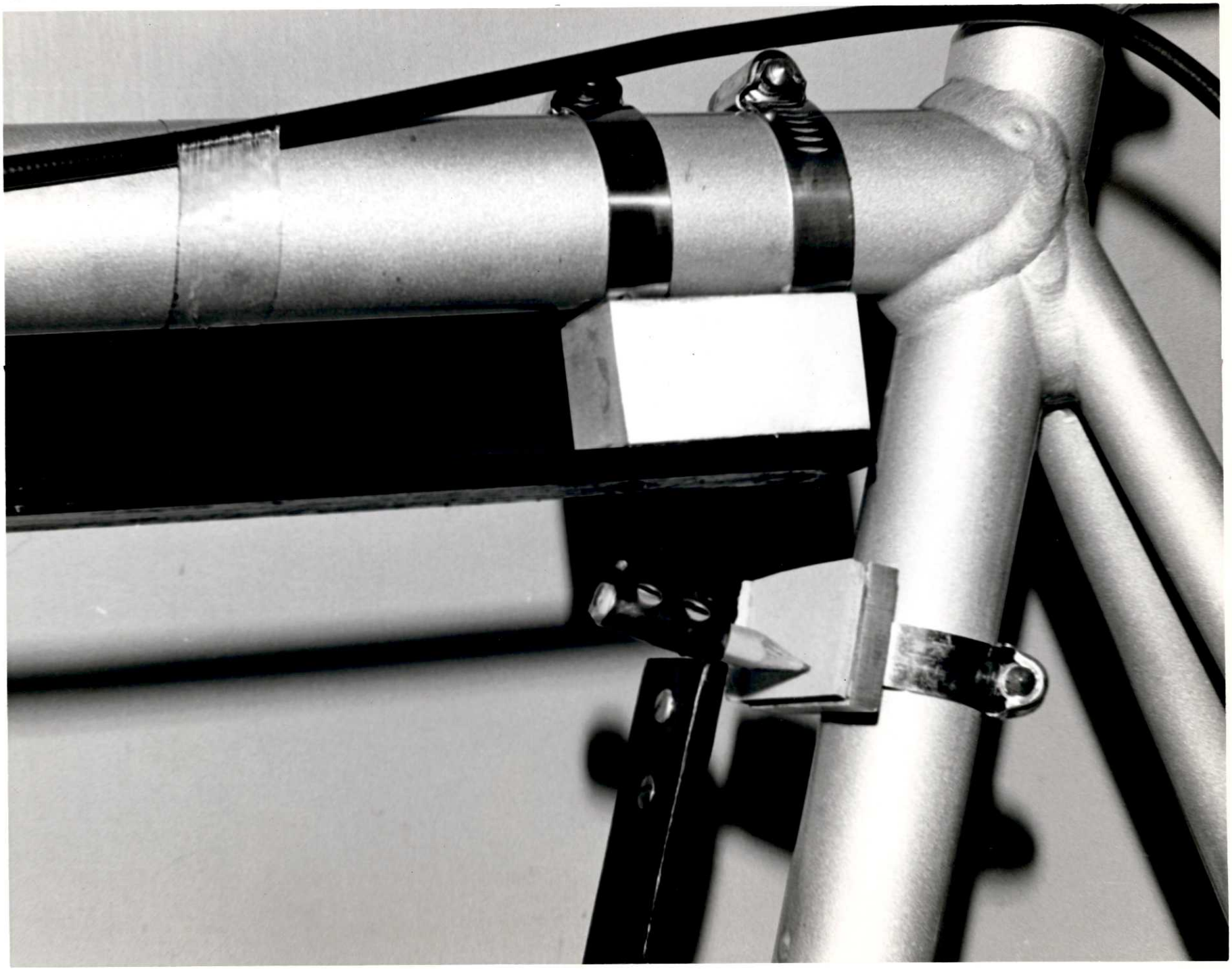

Figure 5 Pointer System



Figure 6 Pointer System

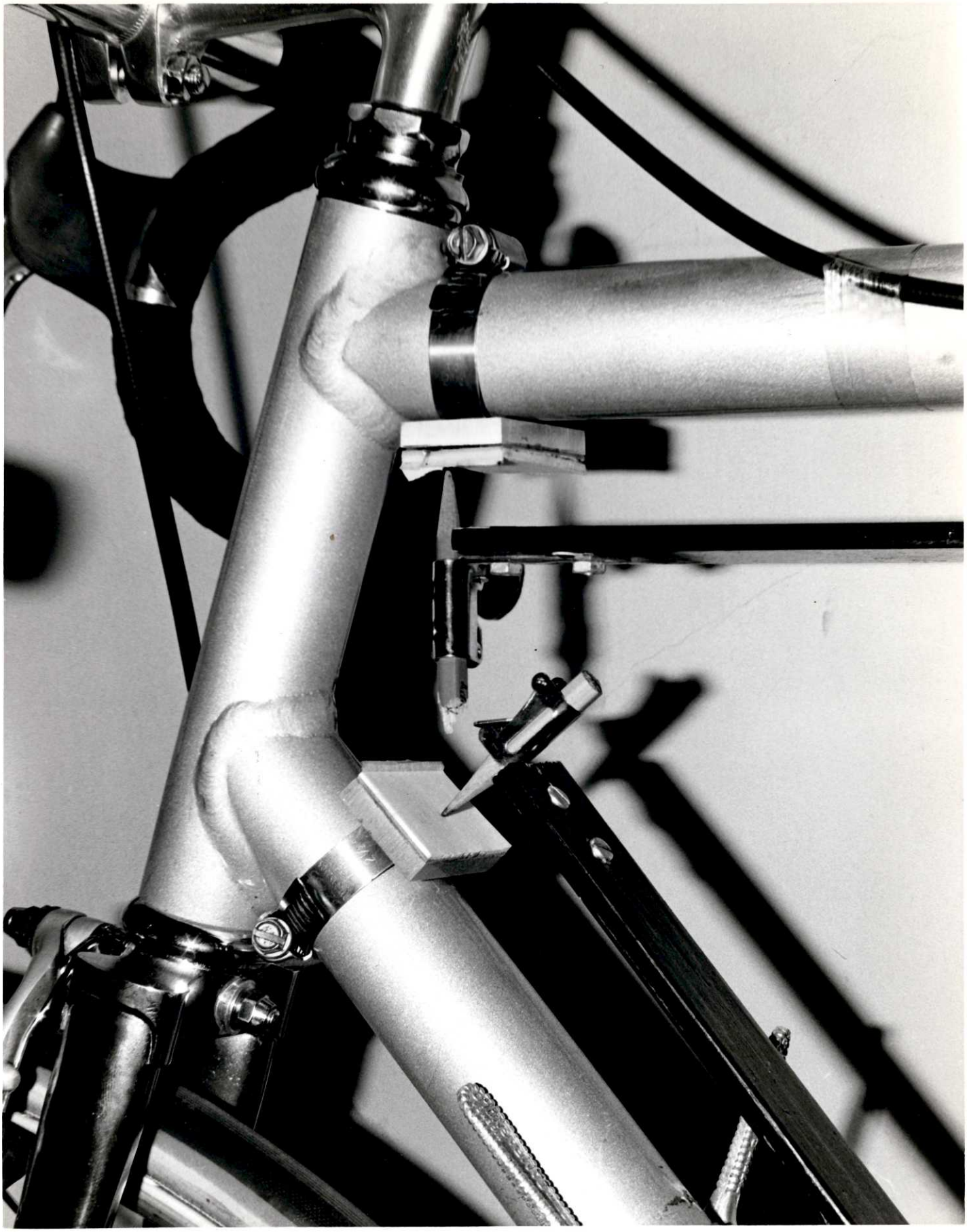

Figure 7 Pointer System

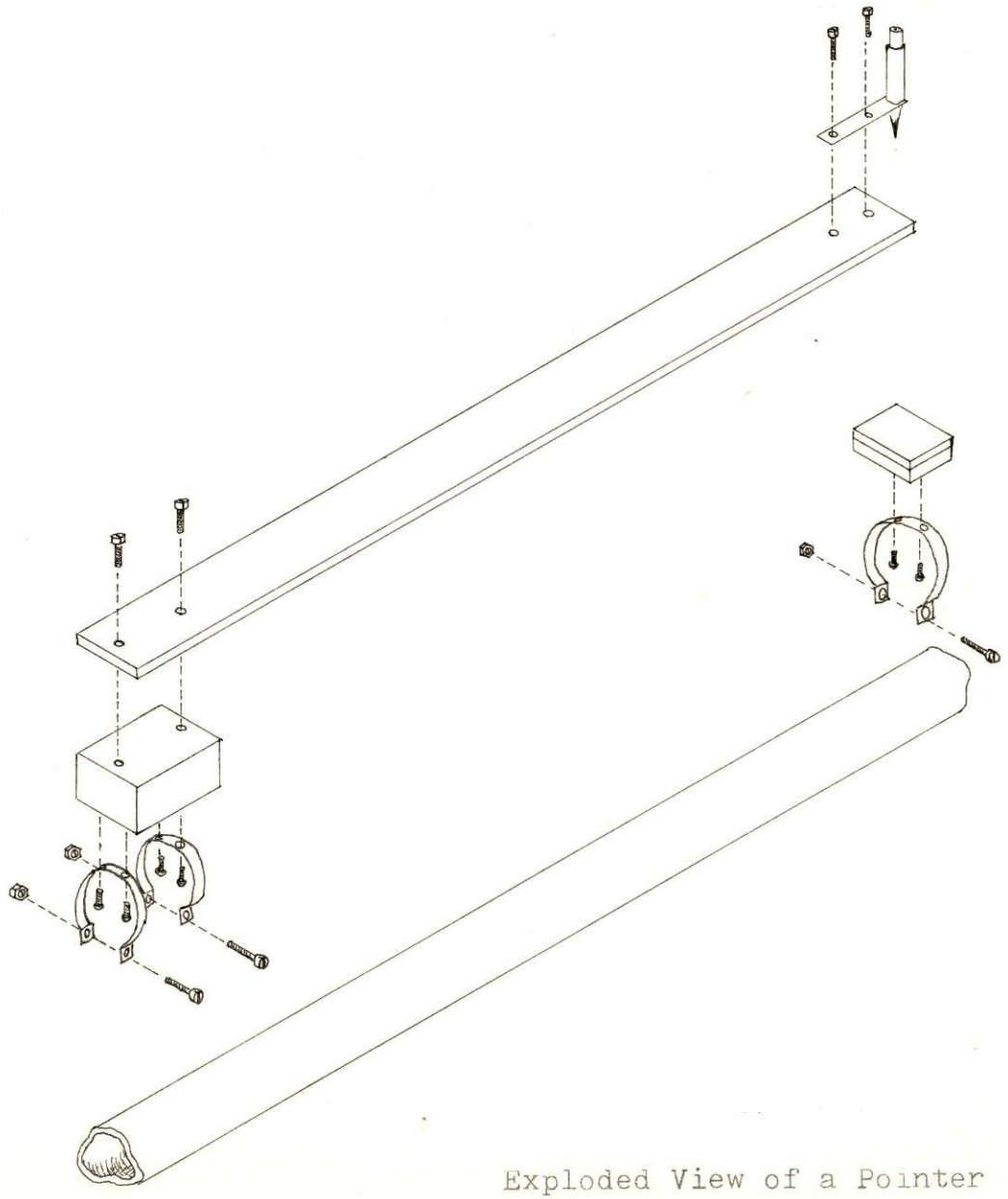

Exploded View of a Pointer

Figure 8

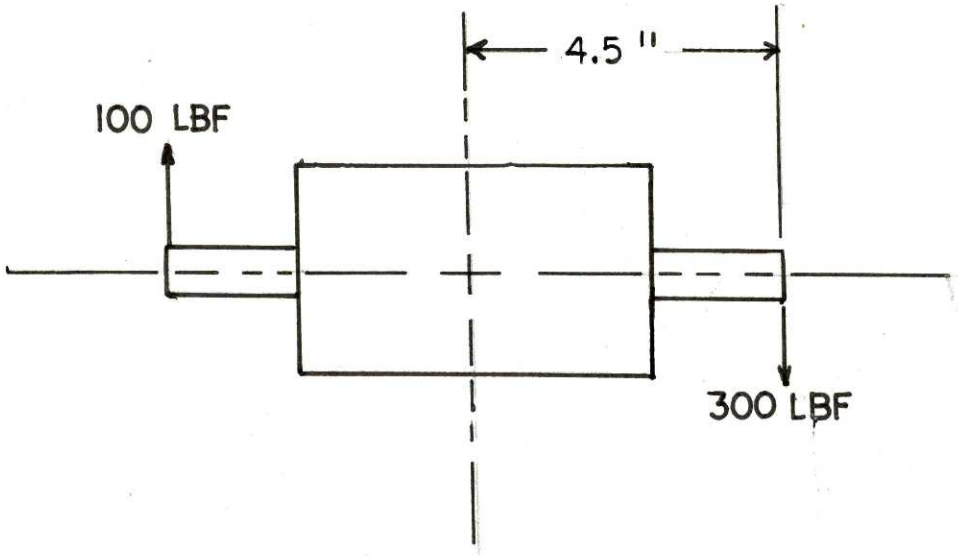

Rider Effected Loading
of the Bottom Bracket

Figure 9a

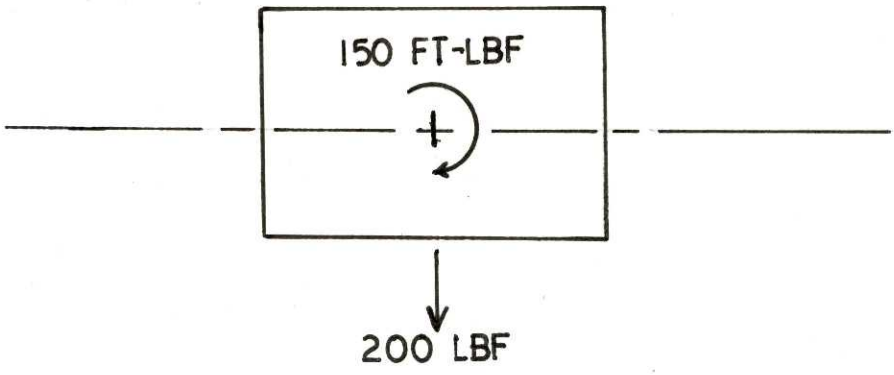

Machine Effected Load
of the Bottom Bracket

Figure 9b

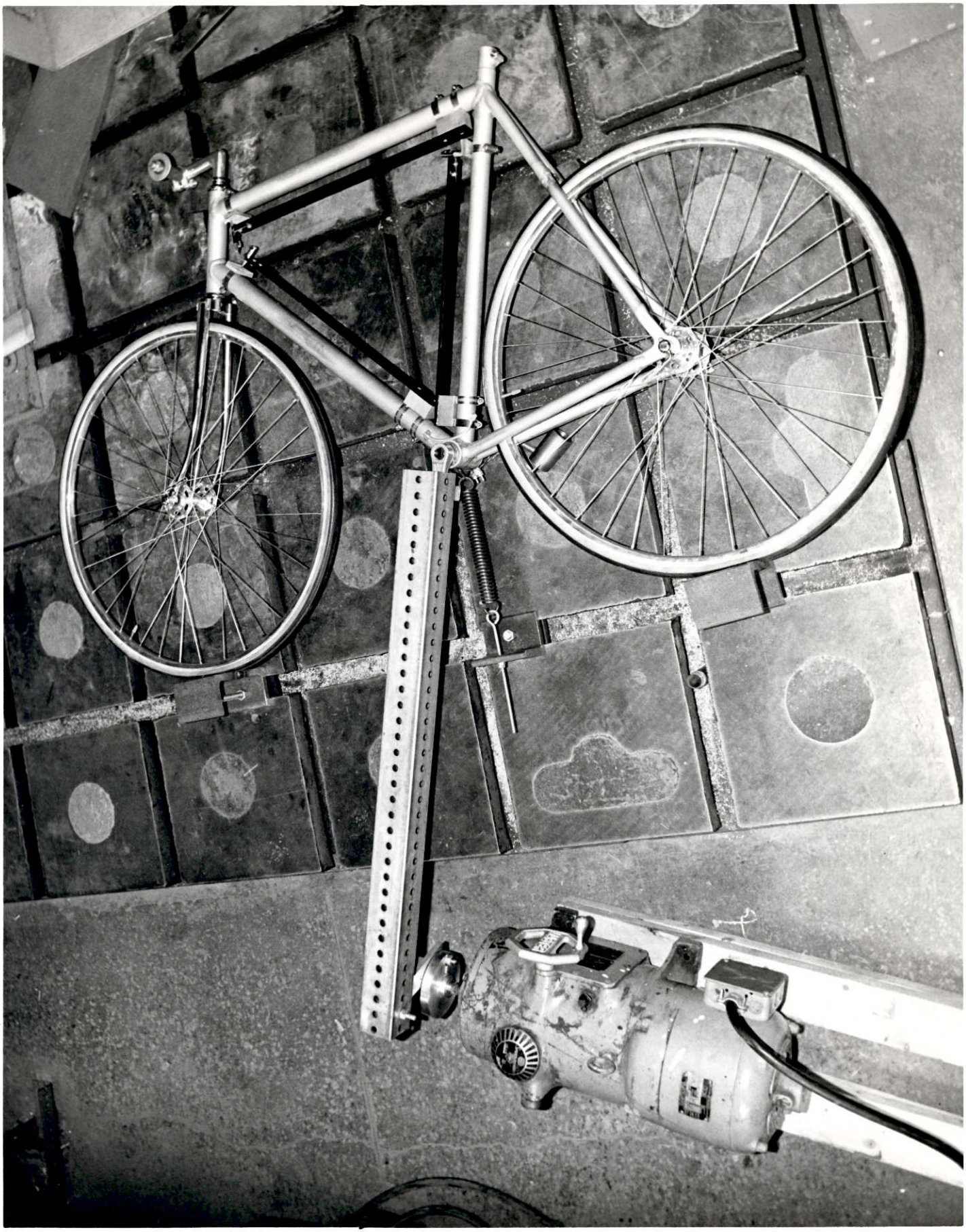

Figure 10 Overhead View of Simulator

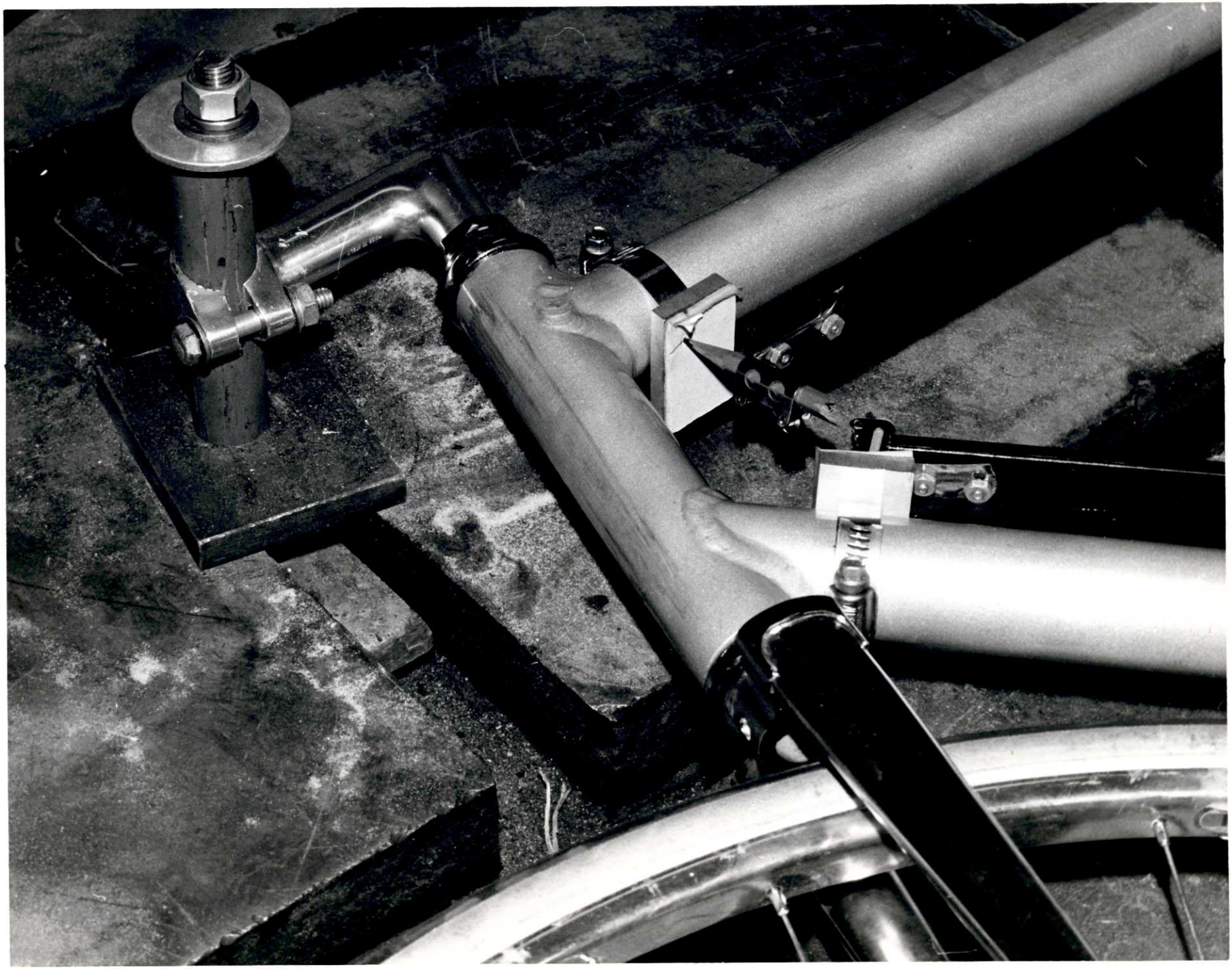

Figure 11 Handlebar Simulation

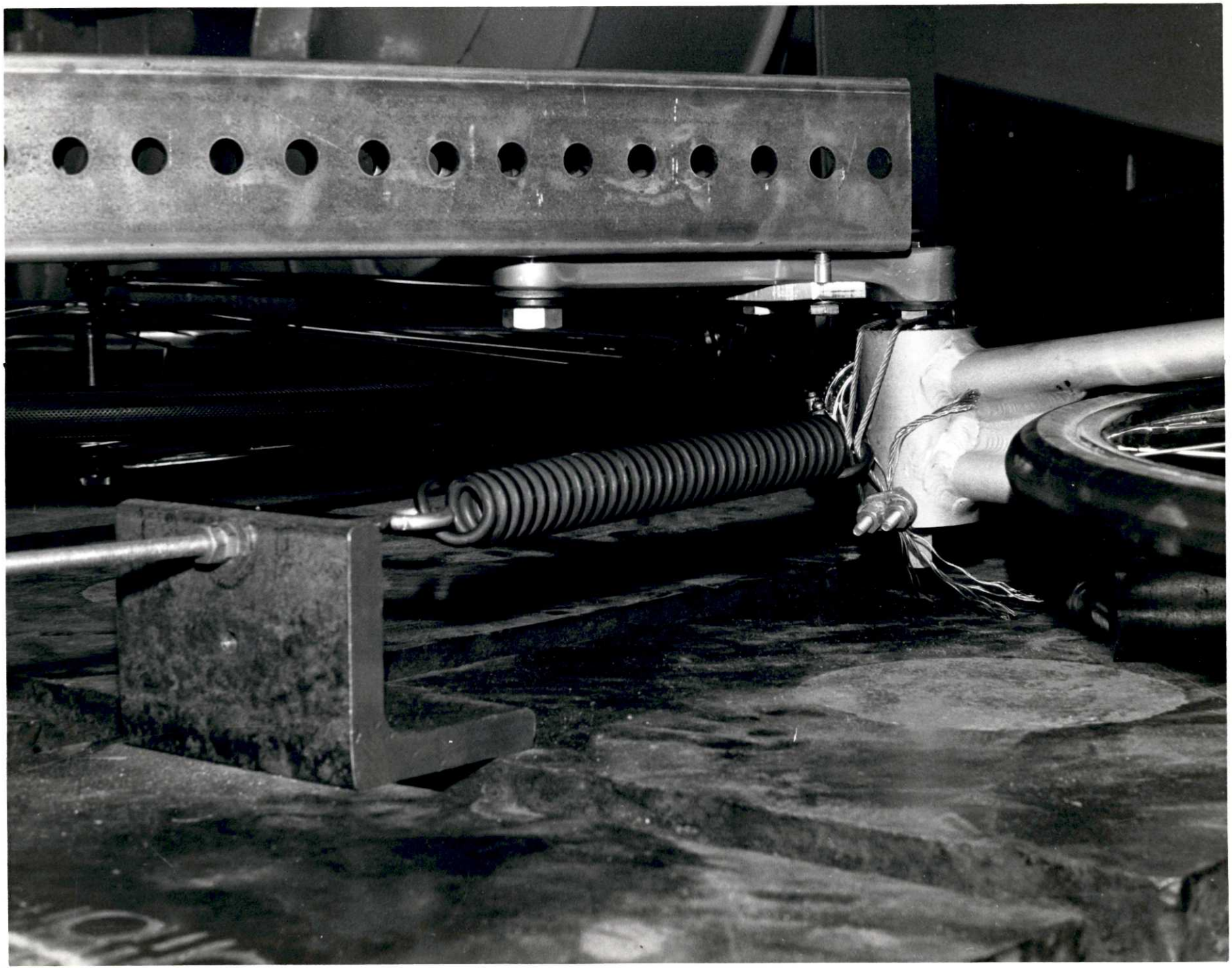

Figure 12 Spring Loading and Lever Arm Attachment

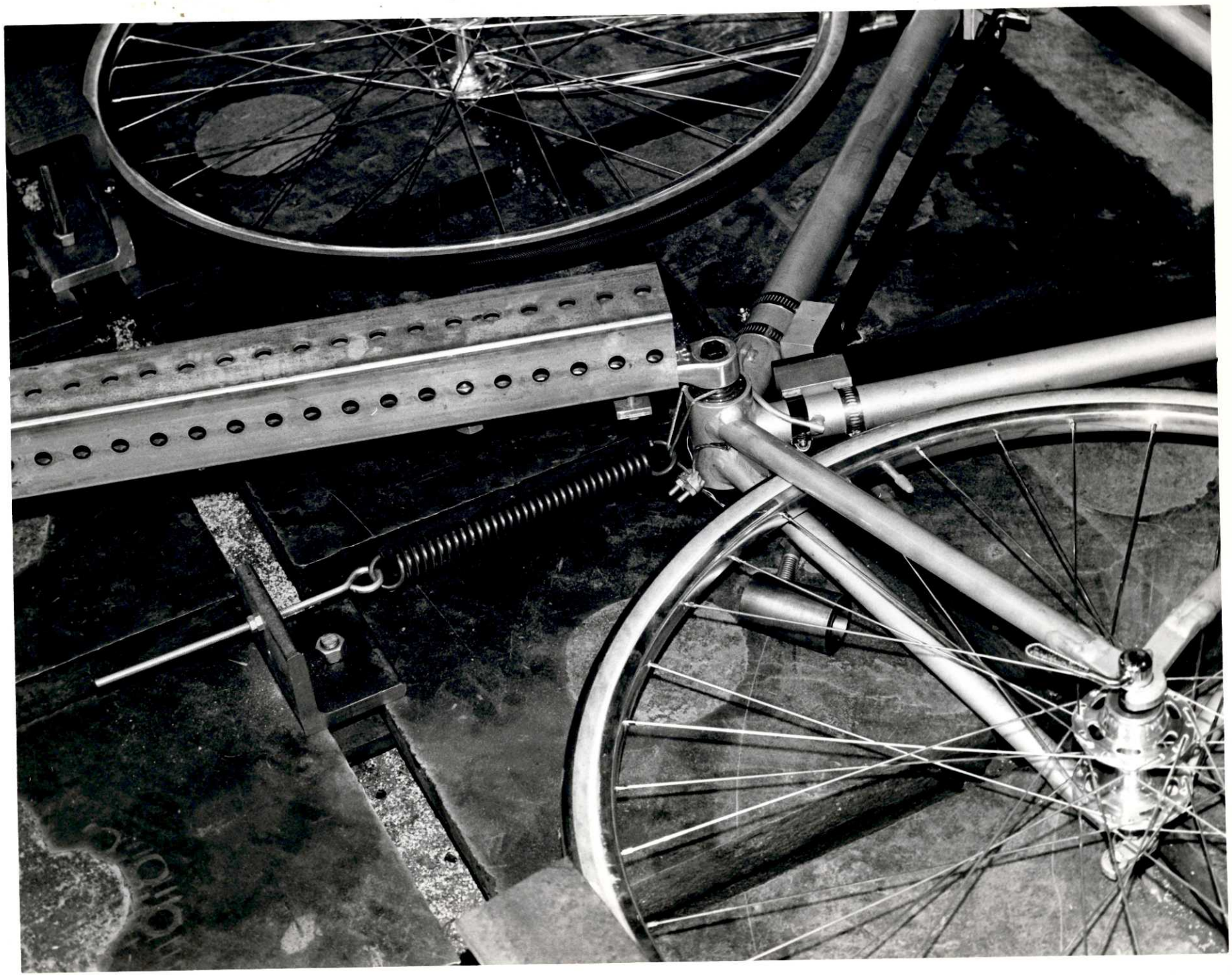

Figure 13 Spring Loading

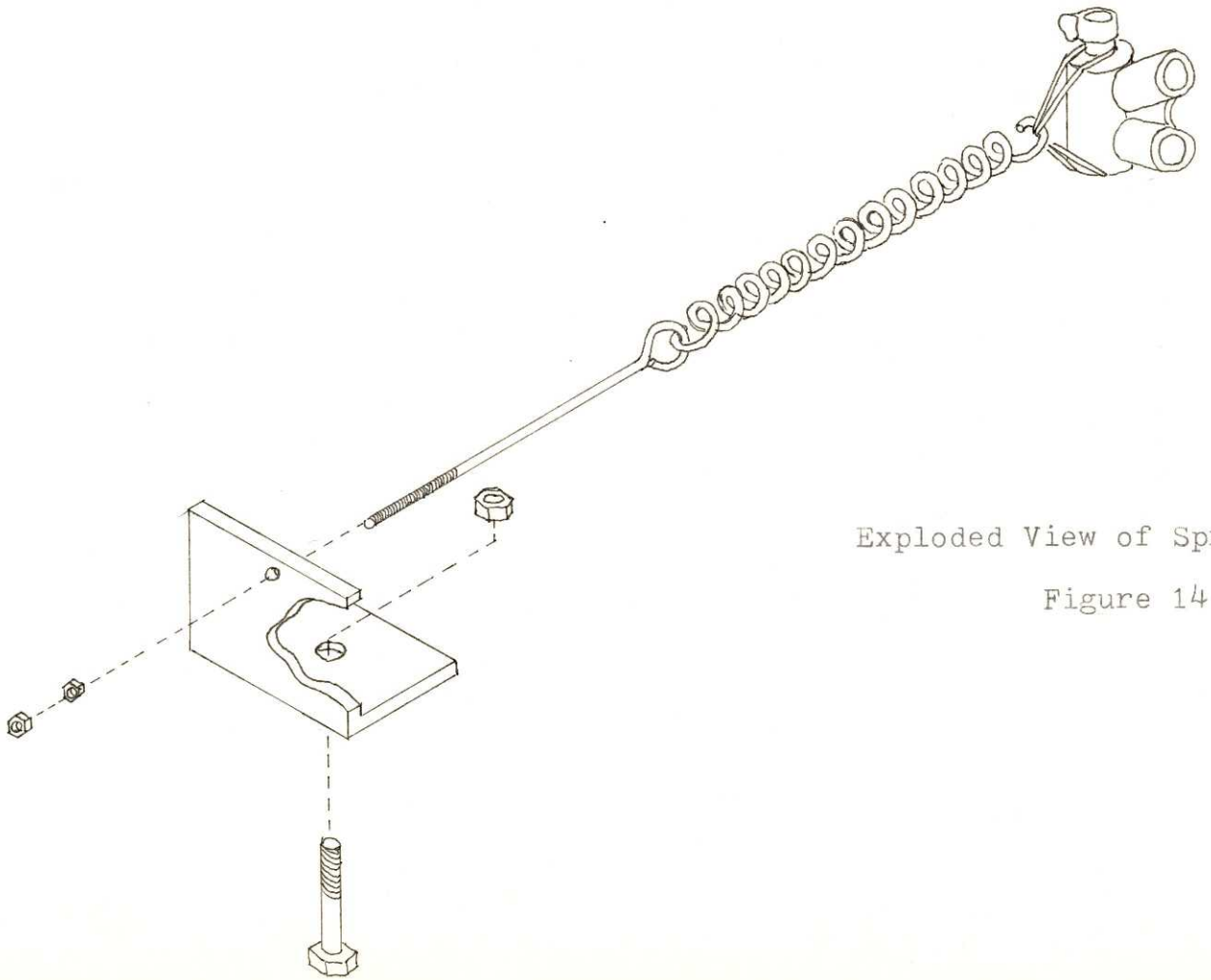

Exploded View of Spring System

Figure 14

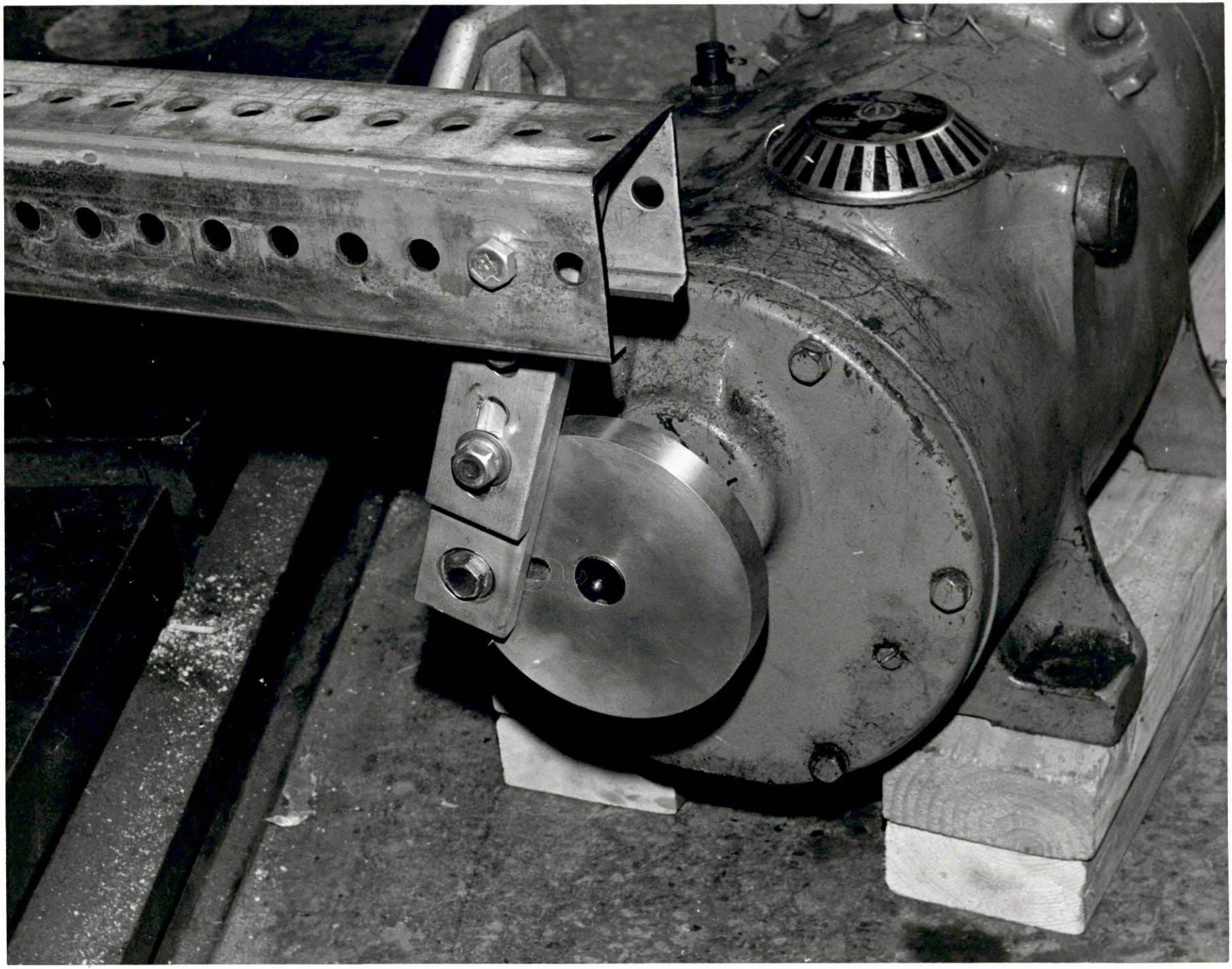

Figure 15 Connecting Rod and Eccentric

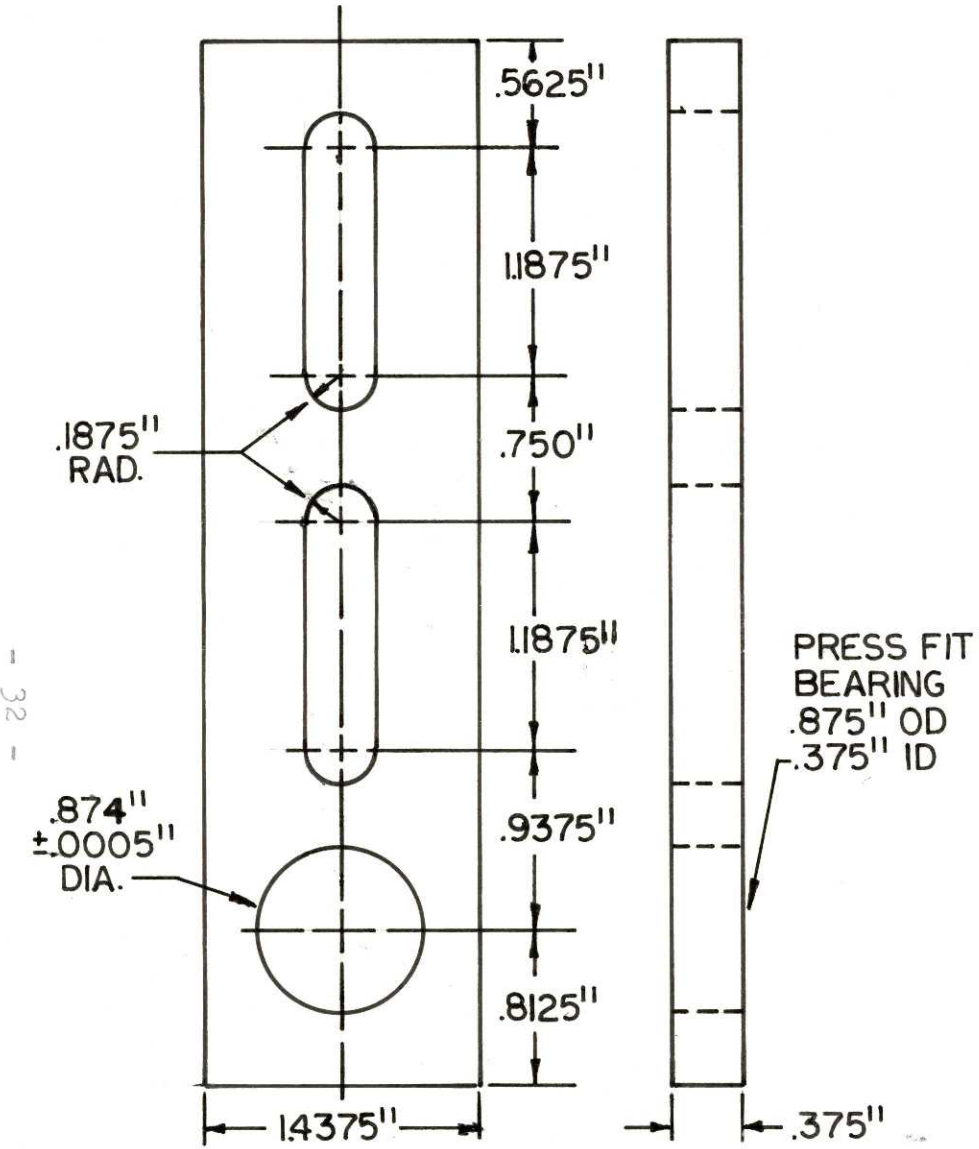

Connecting Rod - Part One

Figure 16

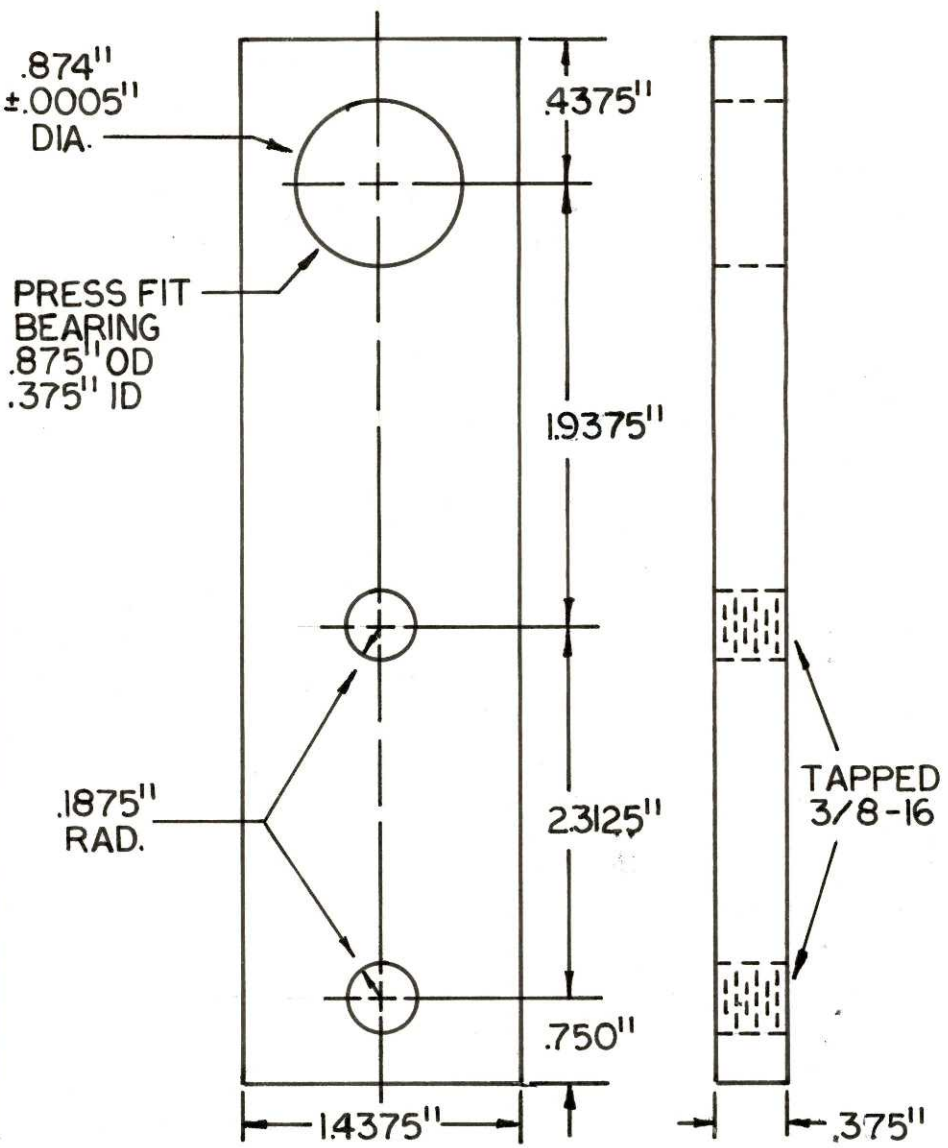

Connecting Rod - Part Two

Figure 17

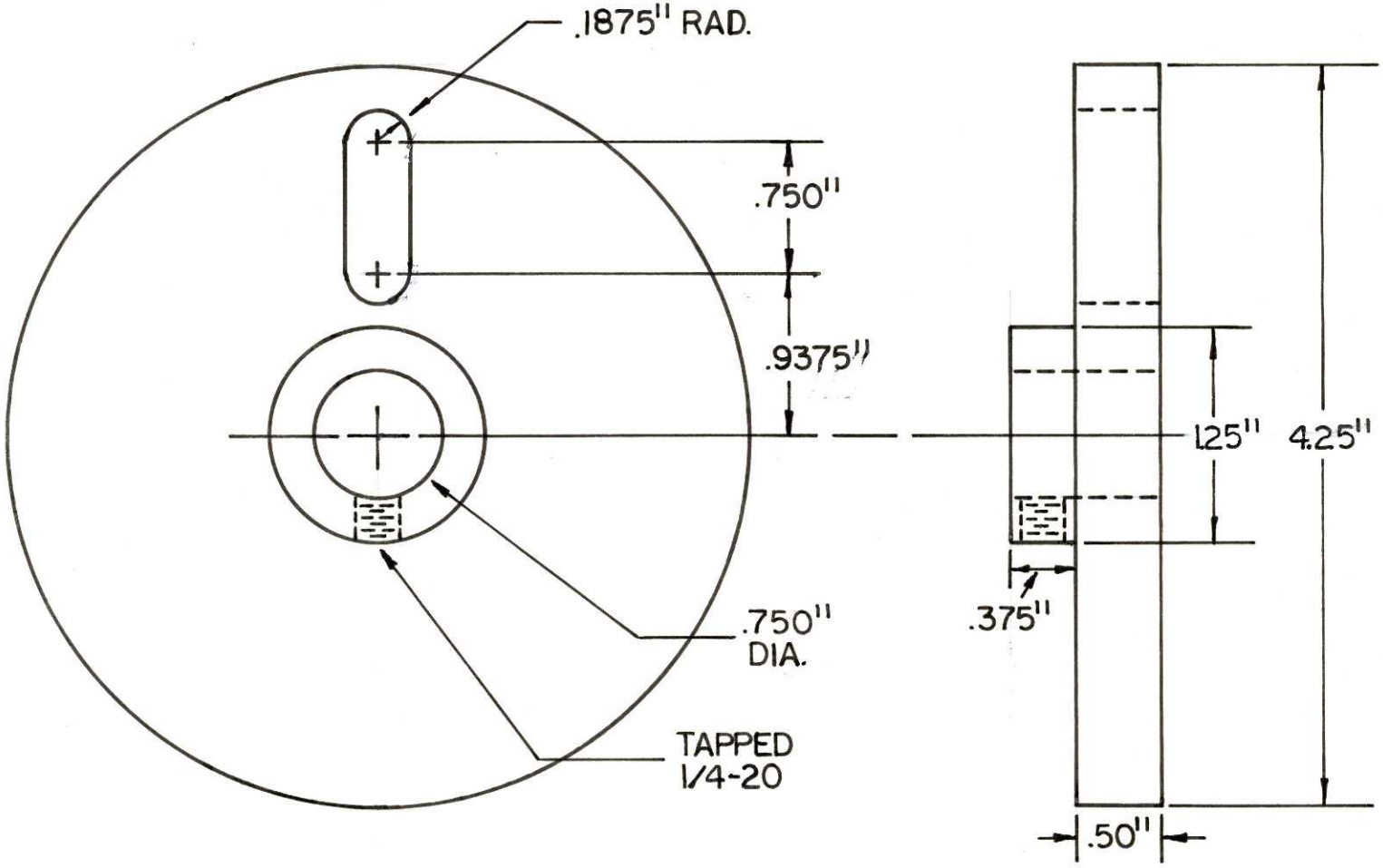

Eccentric

Figure 18

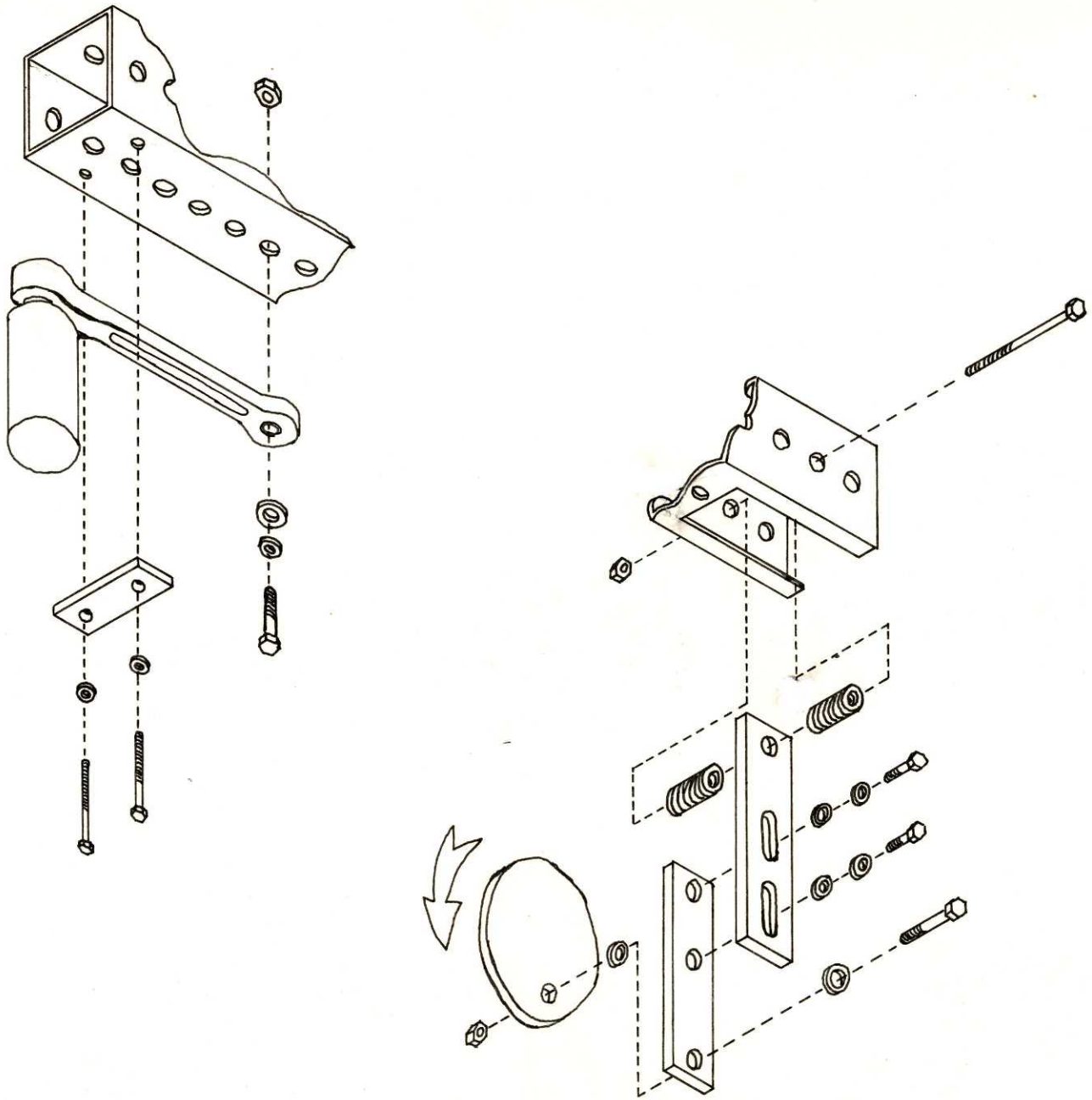

Lever Arm Assembly - Exploded View

Figure 19

APPENDIX 1

Nomenclature

A	Cross-sectional Area
d	Inside Tube Diameter
D	Outside Tube Diameter
E	Young's Modulus
F	Force
ft-lbf	Foot-pound Force
G	Shear Modulus
I_{yy}	Bending Cross-sectional Moment of Inertia
I_z	Twisting Cross-sectional Moment of Inertia
L	Length
lbf	Pound Force
M_b	Bending Moment
M_o	Moment Applied at Bottom Bracket
M_t	Twisting Moment
N	Number of Cycles to Failure
r	Radius of Eccentricity
t	Time
w	Frequency
Y	Vertical Displacement
ρ	Density
σ_a	Alternating Stress Amplitude
σ_{a_0}	Alternating Stress Amplitude Which Gives a Life N at Zero Mean Stress
σ_m	Mean Stress
σ_u	Ultimate Tensile Strength
θ_b	Angular Slope of Tube Due to Bending Moment
θ_t	Angular Twist of Tube Due to Twisting Moment
δ_b	Deflection Due to Bending
δ_t	Deflection Due to Twisting

APPENDIX 2

Maximum Tube Deflection Analysis

A. Seat Tube

$E = 10^7$ psi
$D = 1.25$ in.
$d = 1.202$ in.
$L = 17$ in.

$$\phi_b = \frac{M_o L}{E I_{yy}} \qquad \text{where} \quad I_{yy} = \frac{\pi (D^4 - d^4)}{64}$$

$$\delta_b = L \sin \phi_b$$

Substituting Gives:

$$\phi_b = 6.7^\circ$$

$$\delta_b = 2.0 \text{ in.}$$

B. Down Tube

$L = 18$ in.
$G = 3.7 \times 10^6$ psi
$D = 1.5$ in.
$d = 1.452$ in.
$\theta = 30^\circ$
$M = M_o \cos\theta$
$M_b^t = M_o \sin\theta$

$$\phi_b = \frac{M_b L}{E I_{yy}}$$

where I_{yy} is as defined previously
$= .0303 \text{ in.}^4$

$$\delta_b = L \sin \phi_b$$

Substituting Gives:

$$\phi_b = 2.2^\circ$$

$$\delta_b = .7 \text{ in.}$$

$$\phi_t = \frac{M_t L}{G I_z} \qquad \text{where } I_z = \frac{\pi (D^4 - d^4)}{32}$$

$$= .0606 \text{ in.}^4$$

Substituting Gives:

$$\phi_t = 5^o$$

$$\delta_t = L \sin \phi_t$$

$$\delta_t = 1.7 \text{ in.}$$

$$\delta_{total} = \delta_b + \delta_t$$

$$\delta_{total} = 2.4 \text{ in.}$$

APPENDIX 3

Power Requirement Analysis

The most significant power sink is the lever arm acceleration. This analysis assumes that the motor to be employed is not a reversible transducer.

x = distance along the lever arm measured from the axle in the bottom bracket
L_1 = lever arm length, 36 in.
Y_1 = vertical displacement of the point in consideration on the lever arm
w = 3 cps
r = 2 in.
F_1 = force required to accelerate lever arm
F_2 = force required to deflect frame

(F_1 and F_2 will be of opposite signs since the springiness of the frame is always aiding the motor in accelerating the lever arm in the proper direction)

$$Y_1(x,t) = \frac{xr \sin wt}{L} \qquad \ddot{Y}_1(x,t) = -w^2 Y_1(x,t)$$

$$\frac{dF_1}{dx} = \rho A \ddot{Y}_1(x,t) \qquad \text{where } A = 1.1875 \text{ in.}^2$$

$$\rho = 489 \text{ lbm/ft.}^3$$

$$F_1 = \int_{x=0}^{L} \frac{dF_1}{dx}\, dx$$

Substituting and Integrating Gives:

$F_1 = -11 \sin wt$ lbf

$F_2 = 150 \sin wt$ ft-lbf/ 3 ft
$= 50 \sin wt$ lbf

P = Torque • w
= 39 sin wt • 2 in. • 6 π rad/sec

$P_{avg} = .1$ hp

BIBLIOGRAPHY

Baumeister, Theodore. Mark's Standard Handbook for Mechanical Engineers. New York, McGraw-Hill, 1967

Crandall, Norman C. and Others. An Introduction to the Mechanics of Solids. New York, McGraw-Hill, 1972

Suh, Nam P. and Turner. Elements of the Mechanical Behavior of Solids. M.I.T. Class Notes - 2.30, 1974

Van Horn, Kent R. Aluminum., volumes I and II Pittsburgh, American Society for Metals, 1972